Available online at www.sciencedirect.com
ScienceDirect
Cement and Concrete Research 38 (2008) 77–88
Cement and Concrete Research

Application of the Poisson–Nernst–Planck equations to the migration test☆

K. Krabbenhøft [a,*], J. Krabbenhøft [b]

[a] Centre for Geotechnical and Materials Modelling, University of Newcastle, NSW, Australia
[b] Department of Civil Engineering, Technical University of Denmark, Lyngby, Denmark

Received 30 June 2006; accepted 13 August 2007

Abstract

The Poisson–Nernst–Planck (PNP) equations are applied to model the migration test. A detailed analysis of the equations is presented and the effects of a number of common, simplifying assumptions are quantified. In addition, closed-form solutions for the effective chloride diffusivity based on the full PNP equations are derived, a number of experiments are analyzed in detail, and a new, truly accelerated migration test is proposed. Finally, we present a finite element procedure for numerical solution of the PNP equations.

Keywords: Migration test; Poisson-Nernst-Planck; PNP; Cement; Chloride; Diffusion; Electro-diffusion; Analytical solution; Numerical analysis

1. Introduction

The migration test offers a convenient alternative to natural diffusion tests for determining effective diffusivities for ion transport through saturated porous materials. The combination of chloride ions and cement based materials has, for obvious reasons, been of particular interest. Historically, one of the earliest publications on the methodology was that of Goto and Roy [1] in 1981. Since then, the experimental procedures have evolved a great deal and many advanced techniques have become standard practice. On the other hand, the mathematical models describing the transport of ions under the combined influence of concentration gradients and an electric field have essentially remained unchanged since the test was first proposed. Thus, it is common practice to consider only the transport of the ion in question (usually chloride) and to approximate the electric field by a constant equal to the electric potential change over the sample divided by the sample length. This model, which we will refer to as the conventional single-species model, comes in a transient and a steady-state version, both of which have been used as a basis for estimating the effective chloride diffusivity. A summary of these models and the related experimental procedures can be found in [2,3].

More recently, Samson and co-workers [4–6] have advocated the use of the Poisson-Nernst-Planck (PNP) equations for describing the transport of ions and the distribution and evolution of the electric field. A separate conservation equation is here considered for each ionic species and, in addition, Poisson's equation (i.e. Maxwell's first law or Gauss's law for the electric field) is imposed, effectively coupling the transport of the individual ions. This approach was also followed by Truc et al. [7] where significant differences were found between the full PNP model and the conventional single-species model. In particular, it was found that the composition of the pore solution influences the results significantly. The PNP equations are considerably more complicated than the conventional single-species model and have, perhaps for this reason, not achieved widespread use. Furthermore, since the latter model appears as a special case of the former (namely that where only a single ion is considered and Poisson's equation is ignored) it could perhaps be expected that the difference between the two models would be relatively minor. Although this under some conditions is true, the difference between the two models is often so great that it in our opinion is questionable to even consider one a simplification of the other. For example, the two models may under realistic conditions predict very different concentration profiles. The evolution of these with time can also be quite dissimilar. Furthermore, the constant field approximation may occasionally (though again under realistic conditions) be a very poor approximation. However, in a rather odd twist of circumstances, it turns out that even with these fundamental differences,

☆ Dedicated to Sven Krabbenhøft on the occasion of his 60th birthday.
* Corresponding author.
E-mail address: kristian.krabbenhoft@newcastle.edu.au (K. Krabbenhøft).

0008-8846/$ - see front matter © 2007 Elsevier Ltd. All rights reserved.
doi:10.1016/j.cemconres.2007.08.006

the effective diffusivities predicted by the two models will in many cases be much more similar than it would be reasonable to expect, the differences between the physical characteristics predicted by the two models taken into consideration. This of course explains the fact that numerous researchers over the years have been able to extract effective diffusivities which are in good agreement with what can be obtained using for example natural diffusion tests.

The aim of this paper is to draw attention to the differences between the conventional single-species model and the more complete and therefore (it should be expected, though perhaps naïvely) also more correct PNP model. The purpose of such an exercise is two-fold. First of all, even though the simplified model in many cases does give reasonable estimates of effective diffusivities, its predictions regarding the physical mechanisms of the processes may be quite erroneous which, needless to say, is fundamentally unsatisfactory. Secondly, it is well known that the transport of ions through saturated cement pastes is affected by a number of non-standard phenomena, i.e. mechanisms that can not be accounted for by any known macroscopic model, including the PNP equations. Such anomalies were already observed by Goto and Roy [1] and have since been effectively demonstrated by Yu, Page et al. [8,9].Typically, the anomaly consists of a certain ionic species being much less mobile, i.e. having a much lower effective diffusivity, than would be expected. This is often attributed to the influence of electric doubles layers, an effect that becomes more dominant as the average pore size decreases. However, regardless of the physical mechanisms responsible for this unexpected behaviour, it seems reasonable to initiate the investigations of possible microscopic second-order effects from the most complete macroscopic models available.

To facilitate a systematic comparison between the PNP equations and the conventional single-species model we have attempted to solve the PNP equations analytically whenever possible. For the steady state we obtain a complete solution for the case of a system of an arbitrary number of monovalent ions. This solution is essentially identical to that of Goldman [10] although several simplifications, relating particularly to the setup of typical migration tests, are possible. As a by product of the analytical solution, we derive a simple, closed form expression for the effective diffusivities of the ions in such a system. As for transient solutions, important insights into the qualitative behaviour are also obtained and in the special case of a system of two monovalent ions, a semi-analytical solution is proposed. For the general case, we have to resort to numerical methods and a complete nonlinear finite element procedure is constructed for this purpose.

2. The conventional single-species model (SSM)

The most popular model for describing the transport of chloride ions under the influence of concentration and electric potential gradients is derived using the following chain of arguments. First, in the absence of electric potential gradients, the mass flux of chloride is given by Fick's law as

$$j = -D\frac{\mathrm{dc}}{\mathrm{dx}} \tag{1}$$

where D is the effective diffusion coefficient and c is the concentration. Now, assuming that the sample is placed in an electric circuit, Fick's law should be modified to account for the effect of the resulting electric field. This is done via the Nernst–Planck law so that the flux is given by

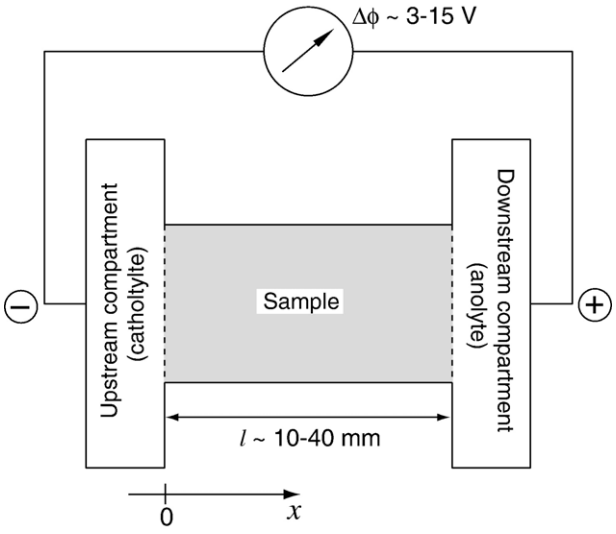

Fig. 1. Migration test.

$$j = \underbrace{-D\frac{\mathrm{d}c}{\mathrm{d}x}}_{\text{Diffusion}} \underbrace{-D\frac{zF}{\mathrm{RT}}c\frac{\mathrm{d}\phi}{\mathrm{d}x}}_{\text{Migration}} \tag{2}$$

Where z is the valence, F is Faraday's constant, R is the ideal gas constant, T is the absolute temperature and ϕ is the electric potential. As indicated in (2), we will refer to the transport resulting from a concentration gradient as diffusion whereas the contribution stemming from the applied electric field is termed migration.

The experiment, see Fig. 1, proceeds by establishing a potential difference between the upstream and downstream compartments and the corresponding electric field is then approximated as

$$\frac{\mathrm{d}\phi}{\mathrm{d}x} \approx \frac{\Delta\phi}{l} = \text{const} \tag{3}$$

where l is the sample length. The flux of chloride ions($z=-1$) is then given by

$$j^- = -D^-\left(\frac{\mathrm{d}c^-}{\mathrm{d}x} - \mathrm{k}c^-\frac{\Delta\phi}{l}\right) \tag{4}$$

where $k=F/(\mathrm{RT})=38.963\ \mathrm{V}^{-1}$ (at 25 °C) has been introduced and superscript "−"(minus) signifies that we a dealing with a negatively charged ion. By requiring mass balance we arrive at the following linear partial differential equation

$$\frac{\partial c^-}{\partial t} - D^-\left(\frac{\partial^2 c^-}{\partial x^2} - k\frac{\Delta\phi}{l}\frac{\partial c^-}{\partial x}\right) = 0 \tag{5}$$

where D^- has been assumed constant. A series solution to this equation has been obtained by Xu and Chanda [12]. It is instructive to liken the governing Eq. (5) to the classical advection diffusion equation (also known as the Burgers equation):

$$\frac{\partial u}{\partial t} - \alpha\frac{\partial^2 u}{\partial x^2} + \alpha\frac{\partial u}{\partial x} = 0 \tag{6}$$

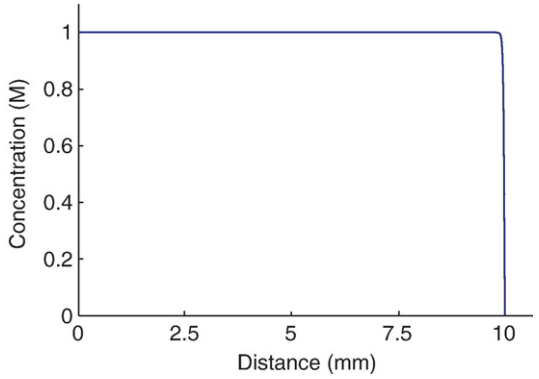

Fig. 2. Concentration profile determined from (5). The profile corresponds to an electric potential difference of $\Delta\phi = 12$ V. The upstream compartment contains a 1 M chloride solution and the downstream compartment contains distilled water. This setup is identical to the one used in [11].

where a is the advective velocity. A central quantity of this equation is the Péclet number defined by

$$Pe = \frac{a}{\alpha} l \tag{7}$$

Thus, for the equation describing the migration test we have

$$Pe = k\Delta\phi \tag{8}$$

Usually, in migration tests, a potential difference of some 3–15 V is applied and the Péclet number is then of the order $Pe \simeq 100$–600[1]. Under such conditions, the chloride profiles take the form of a sharp front moving through the sample towards a steady state as shown in Fig. 2. Furthermore, since the process is completely dominated by migration, the diffusive term in (2) can be ignored and the flux approximated as

$$j^- \approx D^- k c^- \frac{\Delta\phi}{l} \tag{9}$$

In steady-state migration experiments the flux would be measured and the diffusion coefficient can then be determined as [2]

$$D^- \approx \frac{l}{k\bar{c}^- \Delta\phi} j^- \tag{10}$$

where $\bar{c}^-$ is some representative concentration. As shown in Fig. 1, the concentration is, due to the presence of the electric field, constant over almost the entire sample length and the effective diffusivity is therefore taken as

$$D^- \approx \frac{l}{k c_0^- \Delta\phi} j^- = D_{\mathrm{SSM}} \tag{11}$$

where c_0^- is the concentration in the upstream compartment.

Although the conventional single-species model as described so far appears quite reasonable, it is in fact, as will be discussed in the following sections, highly problematic. In particular, the disregard for electroneutrality has severe consequences.

[1] Interestingly, the Péclet number is independent of the length scale in the sense that it depends only on the potential drop over the sample. In biological systems such drops are often measured in the hundreds of mV and the corresponding Péclet numbers will then be approximately a factor of 10 less than what is seen in typical migration tests.

3. The Poisson–Nernst–Planck (PNP) model

The PNP equations involve a separate mass balance equation for each of the ionic species present, similar to the one introduced for the chloride ion in the previous section. However, the electric potential variation is not postulated *a priori*, but is determined as part of the complete solution. This requires specification of an additional differential equation, namely Poisson's equation (in the current context, Maxwell's first equation or Gauss's law for the electric field).

The equations for the mass flux of the ions are associated with the names of Nernst and Planck and take the following form for a system of n positively charged and n negatively charged ions:

$$j_i^+ = -D_i^+ \left(\frac{\mathrm{d}c_i^+}{\mathrm{d}x} + |z_i^+| k c_i^+ \frac{\mathrm{d}\phi}{\mathrm{d}x} \right), i = 1, \ldots, n \tag{12}$$

$$j_i^- = -D_i^- \left(\frac{\mathrm{d}c_i^-}{\mathrm{d}x} - |z_i^-| \mathrm{k} c_i^- \frac{\mathrm{d}\phi}{\mathrm{d}x} \right), i = 1, \ldots, n \tag{13}$$

Here c_{i}^+ and c_{i}^- represent the concentrations of the positively and negatively charged ions respectively and j_i^+, j_i^- and D_i^+, D_i^- are the mass fluxes and diffusivities associated with these ions.

3.1. Steady state response

Requiring mass balance and assuming that both diffusivities are constant leads to the following steady state mass balance equations:

$$\frac{\mathrm{d}^2 c_i^+}{\mathrm{d}x^2} + |z_i^+| k \frac{\mathrm{d}}{\mathrm{d}x} \left(c_i^+ \frac{\mathrm{d}\phi}{\mathrm{d}x} \right) = 0, i = 1, \ldots, n \tag{14}$$

$$\frac{\mathrm{d}^2 c_i^-}{\mathrm{d}x^2} - |z_i^-| k \frac{\mathrm{d}}{\mathrm{d}x} \left(c_i^- \frac{\mathrm{d}\phi}{\mathrm{d}x} \right) = 0, i = 1, \ldots, n \tag{15}$$

These are supplemented with Poisson's equation:

$$\epsilon \frac{\mathrm{d}^2 \phi}{\mathrm{d}x^2} + F \left[\sum_{i=1}^{n} \left(|z_i^+| c^+ - |z_i^-| c^- \right) + \rho \right] = 0 \tag{16}$$

where ϵ is the absolute permittivity and ρ is the fixed charge density. In this paper we will assume that the fixed charge density is negligible. Furthermore, following the analyses presented by MacGillivray [13] and Samson et al. [4], we can for the applications considered here be relatively confident that the first term in (16) is negligible in comparison to the second term (note that $F/\epsilon = \mathrm{O}(10^{15})$ Vm/mol or larger so that very small length scales or very large electric potentials are necessary in order for the first term to have an influence). However, in Appendix A we verify this supposition by numerical solution of the full set of equations for finite values of ϵ.

With these two assumptions ($\rho = 0$ and $\epsilon = 0$), Poisson's equation reduces to that of requiring eletroneutrality:

$$\sum_{i=1}^{n} \left(|z_i^+| c^+ - |z_i^-| c^- \right) = 0 \tag{17}$$

We should note here that an alternative zero-current condition sometimes is imposed. With appropriate boundary conditions, this is equivalent to the electroneutrality condition [14]. In this paper, however, we will deal directly with the condition (17). The governing Eqs. (14), (15), and (17) are amenable to exact solution. To simplify the derivations we will in the following only consider systems of monovalent ions, i.e.

$$|z_i^+| = |z_i^-| = 1 \tag{18}$$

Furthermore, we will only consider the following Dirichlet boundary conditions:

$$\begin{aligned} &c_i^+(x=0) = c_{i,0}^+, i = 1,\dots,n \\ &c_i^+(x=l) = c_{i,l}^+, i = 1,\dots,n \\ &c_i^-(x=0) = c_{i,0}^-, i = 1,\dots,n \\ &c_i^-(x=l) = c_{i,l}^-, i = 1,\dots,n \\ &\phi(x=0) = \phi_0 \\ &\phi(x=l) = \phi_l \end{aligned} \tag{19}$$

In solving the governing equations we first use (17) to write

$$c = \sum_{i=1}^{n} c_i^+ = \sum_{i=1}^{n} c_i^- \tag{20}$$

All conservation equations are then added to yield

$$2\frac{\mathrm{d}^2 c}{\mathrm{d}x^2} = 0 \tag{21}$$

with the solution

$$c(x) = c_0 + \frac{x}{l}\Delta c \tag{22}$$

where

$$c_0 = \sum_{i=1}^{n} c_{i,0}^+ = \sum_{i=1}^{n} c_{i,0}^-,\ c_l = \sum_{i=1}^{n} c_{i,l}^+ = \sum_{i=1}^{n} c_{i,l}^-, \tag{23}$$

$$\Delta c = c_l - c_0$$

Note that, for a system of system of two monovalent ions, the linear concentration profiles predicted by the PNP equations are in stark contrast to those of the conventional single-species model shown in Fig. 2. Next, the mass conservation equations relating to negatively charged ions are summed and subtracted from the sum of the equations governing the transport of positively charged ions. This gives

$$2\frac{\mathrm{d}^2 c}{\mathrm{d}x^2} + 2k\frac{\mathrm{d}}{\mathrm{d}x}\left(c\frac{\mathrm{d}\phi}{\mathrm{d}x}\right) = 0 \tag{24}$$

With $c(x)$ known the electric potential distribution can be determined as

$$\phi(x) = \phi_0 + \frac{\ln\left(1 + \frac{\Delta c}{c_0}\frac{x}{l}\right)}{\ln(c_l/c_0)}\Delta\phi \tag{25}$$

where

$$\Delta\phi = \phi_l - \phi_0 \tag{26}$$

With $\phi(x)$ known, each mass conservation equation can then be solved for the species concentrations, the result being

$$\begin{aligned} c_i^{\pm}(x) = {} & \frac{c_{i,0}^{\pm} c_l^{\pm\alpha} - c_{i,l}^{\pm} c_0^{\pm\alpha}}{c_0 c_l^{\pm\alpha} - c_l c_0^{\pm\alpha}}\left(\frac{x}{l}\Delta c + c_0\right) \\ & - \frac{c_{i,0}^{\pm} c_l - c_{i,l}^{\pm} c_0}{c_0 c_l^{\pm\alpha} - c_l c_0^{\pm\alpha}}\left(\frac{x}{l}\Delta c + c_0\right)^{\pm\alpha} \end{aligned} \tag{27}$$

where

$$\alpha = \frac{k\Delta\phi}{\ln(c_0/c_l)} \tag{28}$$

These expression for the concentration profiles can be simplified by observing that

$$\lim_{\alpha\to\infty} \frac{c_{i,0}^{+} c_l^{\alpha} - c_{i,l}^{+} c_0^{\alpha}}{c_0 c_l^{\alpha} - c_l c_0^{\alpha}} = \frac{c_{i,l}^{+}}{c_l} \tag{29}$$

and

$$\lim_{\alpha\to\infty} \frac{c_{i,0}^{-} c_l^{-\alpha} - c_{i,l}^{-} c_0^{-\alpha}}{c_0 c_l^{-\alpha} - c_l c_0^{-\alpha}} = \frac{c_{i,0}^{-}}{c_0} \tag{30}$$

For typical migration tests where $\alpha \simeq 100-600$, these approximations are very good indeed. We thus have

$$c_i^+(x) = \frac{c_{i,l}^+}{c_l}\left(\frac{x}{l}\Delta c + c_0\right) - \frac{c_{i,l}^+ c_l - c_{i,l}^+ c_0}{c_0 c_l^{\alpha} - c_l c_0^{\alpha}}\left(\frac{x}{l}\Delta c + c_0\right)^{\alpha} \tag{31}$$

$$\begin{aligned} c_i^-(x) = {} & \frac{c_{i,0}^-}{c_0}\left(\frac{x}{l}\Delta c + c_0\right) \\ & - \frac{c_{i,0}^- c_l - c_{i,l}^- c_0}{c_0 c_l^{-\alpha} - c_l c_0^{-\alpha}}\left(\frac{x}{l}\Delta c + c_0\right)^{-\alpha} \end{aligned} \tag{32}$$

By taking similar limits, the fluxes are given by[2]

$$j_i^- = -D_i^- \frac{\Delta c}{l}\frac{c_{i,0}^-}{c_0}(1+\alpha) \tag{33}$$

$$j_i^+ = -D_i^+ \frac{\Delta c}{l}\frac{c_{i,l}^+}{c_l}(1-\alpha) \tag{34}$$

Finally, we can obtain an expression for the effective chloride diffusivity in a system containing an arbitrary number of monovalent ions:

$$D_i^- = \frac{l}{\Delta c}\frac{c_0}{c_{i,0}^-}\frac{1}{1+\alpha} j_i^- = D_{\mathrm{PNP}} \tag{35}$$

[2] Again, these are very good approximations – for typical conditions under which migration tests are performed, the error is outside the range of double precision arithmetic, i.e. of order 10^{-16} or smaller.

This diffusivity may be expressed in several alternative ways, for example:

$$D_{\mathrm{PNP}} = \frac{\ln(c_0/c_l)}{(1-c_l/c_0)(1+1/\alpha)} D_{\mathrm{SSM}} \tag{36}$$

or

$$D_{\mathrm{PNP}} = \frac{k\Delta\phi}{(1-c_l/c_0)(1+\alpha)} D_{\mathrm{SSM}} \tag{37}$$

By noting that usually $\alpha \gg 1$ we obtain the approximation

$$D_{\mathrm{PNP}} \approx \frac{\ln(c_0/c_l)}{1-c_l/c_0} D_{\mathrm{SSM}} = D^*_{\mathrm{PNP}} \tag{38}$$

It easily verified that

$$D^*_{\mathrm{PNP}} \geq D_{\mathrm{SSM}} \tag{39}$$

for $c_0 \geq c_l$, with equality only in the case where $c_0 = c_l$.

3.2. Transient response

The full transient response of the PNP equations cannot, as far as we are aware, be expressed in closed form. However, for the special case of a system of two monovalent ions, important information about the qualitative behavior of the system can be extracted. We may here write the governing equations as

$$\frac{1}{D^+}\frac{\partial c^+}{\partial t} - \frac{\partial^2 c^+}{\partial x^2} - k\frac{\partial}{\partial x}\left(c^+\frac{\partial \phi}{\partial x}\right) = 0 \tag{40}$$

$$\frac{1}{D^-}\frac{\partial c^-}{\partial t} - \frac{\partial^2 c^-}{\partial x^2} + k\frac{\partial}{\partial x}\left(c^-\frac{\partial \phi}{\partial x}\right) = 0 \tag{41}$$

$$c^+ - c^- = 0 \tag{42}$$

Introducing $c = c^+ = c^-$ we have, by addition of (40) and (41),

$$\left(\frac{1}{D^+} + \frac{1}{D^-}\right)\frac{\partial c}{\partial t} - 2\frac{\partial^2 c}{\partial x^2} = 0 \tag{43}$$

or

$$\frac{\partial c}{\partial t} = \overline{D}\frac{\partial^2 c}{\partial x^2} = 0 \tag{44}$$

where

$$\overline{D} = 2\left(\frac{1}{D^+} + \frac{1}{D^-}\right)^{-1} \tag{45}$$

which is a well known result [14,15]. Thus, the process of attaining a steady state will progress a rate which is governed by the effective diffusivity $\overline{D}$ alone, i.e. it will be completely independent of the magnitude of the applied electric field. This may be contrary to intuition and is certainly contrary to what the conventional single-species model predicts. With $c(x,t)$ known, we can in principle solve (40) or (41) for $\phi(x,t)$. To our knowledge, however, these calculations cannot be carried out in closed form and one has to resort to some kind of numerical solution, for example Runge–Kutta integration or, more generally, schemes such as those based on finite differences or finite elements. In the present, the latter option has been preferred and the full finite element scheme (incorporating the complete Poisson equation) is given in Appendix A.

4. System of two monovalent ions

Andrade and co-workers have in several studies used an experimental setup where the upstream compartment contained a solution of NaCl while the downstream compartment contained distilled water [3,11,16]. In all these studies the constant field assumption was used and electroneutrality was ignored. Consequently, in the steady state, the resulting effective chloride diffusion coefficient was computed from (11).

To illustrate the effect of the electroneutrality condition for such a setup, lets see what the PNP equations give. In the case of a system of two monovalent ions we have $i=1$, $c_i^+ = c_i^- = c$, and with the downstream compartment containing distilled water $c_l = 0$. The effective diffusion coefficient is thus given by

$$D_{\mathrm{PNP}} = \frac{l}{c_0} j^- \tag{46}$$

corresponding to a situation where the only transport is that which stems from natural diffusion. From a physical point of view this is of course a result of the electroneutrality condition which effectively requires that a migration of chloride ions be accompanied by an equal and oppositely directed migration of sodium ions. However, since the concentration of sodium in the downstream compartment is zero the chloride is effectively immobile, apart from the natural diffusion contribution. The physical basis of the experiment is thus questionable and it would not be reasonable to expect that any meaningful results could derived from it. Quite surprisingly, however, very good agreement is found between diffusivities determined from this type of migration test and ones determined from natural diffusion tests (see for example [11]). This is most likely due to the fact that the pore solution inevitably will contain a certain amount of

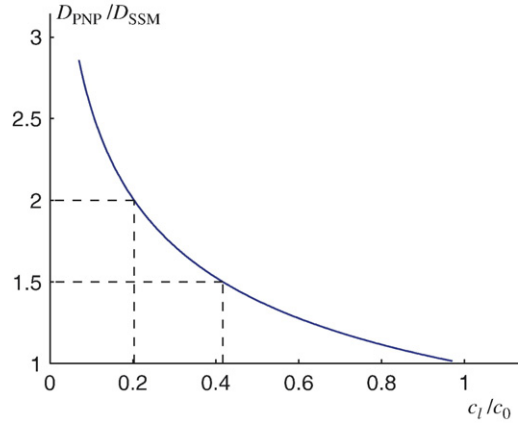

Fig. 3. Ratio between diffusion coefficients as function of the ratio between the chloride concentrations in the downstream and upstream compartments.

Table 1
Setup used for experimental and numerical studies by Samson et al. [6]

$c^+_{Na,0}$	$c^-_{OH,0}$	$c^-_{Cl,0}$	$c^+_{Na,l}$	$c^-_{OH,l}$	$c^-_{Cl,l}$	l[mm]	$\Delta\phi$[V]
0.8	0.3	0.5	0.3	0.3	0.0	35	14

All concentrations are in mol/L.

positively charged ions that can facilitate the transport of chloride under the condition of electroneutrality.

Assuming that a certain amount of NaCl is present in the downstream compartment, we can compare the diffusivities determined from the single-species model to those obtained with the complete PNP model. The ratio D^*_{PNP}/D_{SSM} is plotted in Fig. 3. We here see that a factor of 2 between the two coefficients is obtained already for a relative concentration of $c_0/c_l \simeq 0.2$ whereas an increase to $c_0/c_l \simeq 0.42$ implies a ratio between the two diffusivities of 1.5.

5. Multi-ion systems — NaCl+NaOH

A more common alternative to the experimental setup described above is to first saturate the sample with an alkaline solution and subsequently maintain identical solution concentrations in the up-and downstream compartments. The alkaline is usually a saturated, or near-saturated, solution of $Ca(OH)_2$ [17] or, more commonly, NaOH [6,18]. In the following we will investigate the latter possibility. The inadequacy of the conventional single-species model has previously been noted by Samson et al. [6] who studied a test with the characteristics given in Table 1. For this system we can again derive a ratio between the diffusivities associated with the two models. The boundary concentrations are given by

$$c_0 = c_{NaOH,0} + c_{NaCl,0};\quad c_l = c_{NaOH,l} = c_{NaOH,0} \tag{47}$$

and the ratio between the diffusivities then follows as

$$\frac{D^*_{PNP}}{D_{SSM}} = \frac{\ln(c_0/c_l)}{1 - c_l/c_0} = \left(1 + \frac{c_{NaOH,0}}{c_{NaCl,0}}\right)\ln\left(1 + \frac{c_{NaCl,0}}{c_{NaOH,0}}\right)(>1) \tag{48}$$

For the boundary conditions used by Samson et al. this gives $D^*_{PNP}/D_{SSM}=1.57$. The ratio between the two diffusion coefficients is illustrated in Fig. 4 where we see that the validity of the simplified model depends critically on the ratio between the NaOH and NaCl concentrations.

6. Shape and evolution of concentration profiles

The shape of the chloride profiles and their evolution with time has been the subject of some debate and the issue appears to remain largely unresolved. Tang and Nilsson [17,19] advocate a distribution and evolution following that predicted by the singles-species model, i.e. a front-like evolution of the chloride profile to finally end up with a steady-state as shown in Fig. 2. Experimental evidence to support this supposition is presented. Later on, however, Tang [20] presented experimental evidence that appears to contradict the conventional single-species model. Thus, the variation is much less abrupt than suggested by this model and seem more like the profiles that would result from natural diffusion processes.

This disagreement between theory and experiment has motivated Stanish et al. [21] to formulate a new transport model. The basic idea is here that an individual ion experiences an effective resistance that increases with the distance traveled. This phenomenon is observed in other porous media, notably wood [22,23] where, amongst other things, an apparent sample length dependence can be observed when determining hydraulic conductivities. Thus, although the phenomenon may well be a true anomaly, it is in our opinion natural to first search for an explanation among models that do not require non-standard consideration of length scales.

The PNP equations constitute such a model. On the basis of the analysis of the previous section it is evident that the accuracy of the single-species model gets better as the ratio of NaOH to NaCl increases. This trend also translates over to the shape and evolution of the profiles such that for concentrated NaCl solutions, a diffusion type behaviour is observed whereas, for dilute NaCl solutions, the behaviour is much like that predicted by the conventional single-species model. This point is illustrated in Fig. 5 where the boundary conditions shown in Table 2 have been used. In all cases, the initial state is given by the NaOH concentrations at the ends of the sample.

The simulated profiles reveal that for dilute NaCl solutions, the transport of chloride takes place via a front-like movement

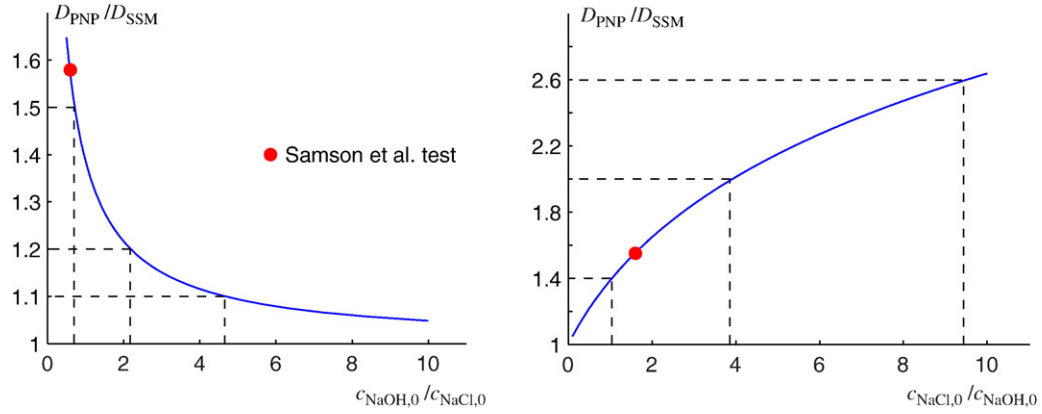

Fig. 4. Ratio (48) between diffusion coefficients computed from the PNP equations and on basis of the conventional single-species model.

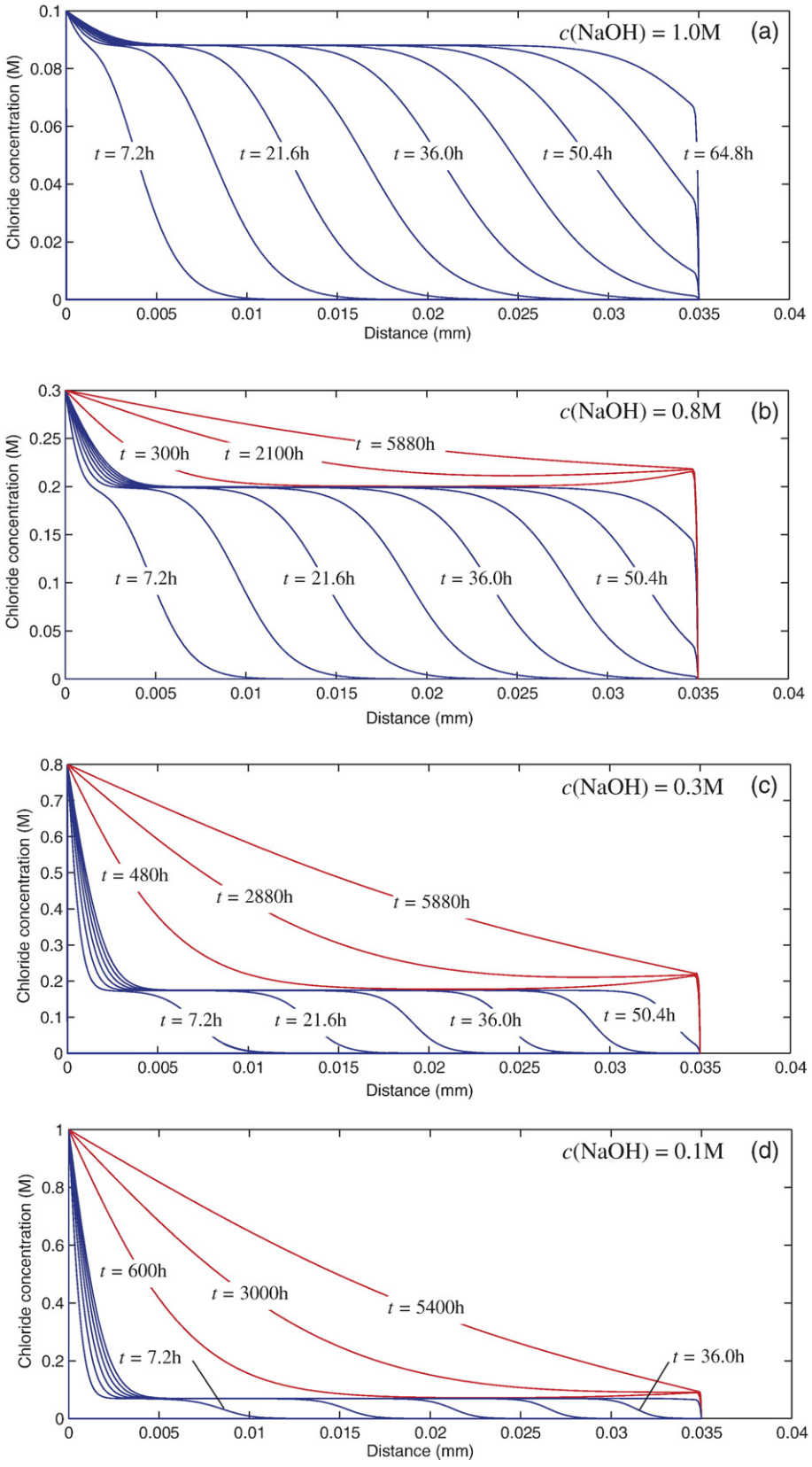

Fig. 5. Simulated chloride concentration profiles.

Table 2
Boundary and initial conditions for simulated experiments shown in Fig. 5(a)(d)

Figure	$c_{\mathrm{NaOH},0}$	$c_{\mathrm{NaCl},0}$	$c_{\mathrm{NaOH},l}$	$c_{\mathrm{NaCl},l}$	$c^{\mathrm{init}}_{\mathrm{NaOH}}$	$c^{\mathrm{init}}_{\mathrm{NaCl}}$	l[mm]	$\Delta\phi$[V]
5(a)	1.0	0.1	1.0	0.0	1.0	0.0	35	14
5(b)	0.8	0.3	0.8	0.0	0.8	0.0	35	14
5(c)	0.3	0.8	0.3	0.0	0.3	0.0	35	14
5(d)	0.1	1.0	0.1	0.0	0.1	0.0	35	14

as predicted by the single-species model. As the concentration of NaCl increases compared to that of NaOH, there is still an initial front-like transport which is followed by a much slower diffusive transport. Obviously, this is again a consequence of positively charged ions being in limited supply so that the mobility of the negatively charged ions effectively is reduced to a value characteristic of natural diffusion. This again illustrates the potentially very significant effects of electroneutrality. In conclusion, it does not seem altogether unreasonable that the apparently anomalous chloride concentration profiles identified by Stanish et al. [21] in part are the result of the particular experimental conditions, i.e. the boundary and initial conditions.

7. A truly accelerated migration test

The whole point of the migration test is of course that it should be much faster to perform than standard natural diffusion tests. However, as shown in the previous section, the time to attain a steady state may, depending on the experimental conditions chosen, be extraordinarily long, i.e. comparable to that of natural diffusion tests. On the other hand, under the right experimental conditions, the test may deliver on its promise of being a rapid way of determining effective diffusivities.

After some experimentation with different initial and boundary conditions, we have come up with the following "optimal" test. The sample is initially saturated with a solution of NaCl. It is here important that the pore solution contains only NaCl, which of course may be difficult to attain. Nevertheless, for the sake of argument, we will assume that it is possible. The sample is then placed in the migration cell where the upstream chamber contains a solution of NaCl of the same concentration as in the sample. The downstream chamber, on the other hand, contains a solution of NaOH, also of a concentration equal to that of NaCl in the sample. In this case we have

$$D_{\mathrm{PNP}} = D_{\mathrm{SSM}} \tag{49}$$

Furthermore, the time to attain a steady state is in the order of minutes rather than hundreds or thousands of hours. The variation with time of the flux at the down stream compartment for a simulated test with the same properties as that in the previous section (except for the boundary and initial conditions) is shown in Fig. 6. The boundary and initial concentrations are 0.5 M. A state which for all practical purposes is steady, is here attained with in the first 20-30 minutes. Except for a small deviation due to natural diffusion, the chloride concentration profile will be as the initial one, i.e. constant throughout the sample to become zero at the downstream compartment.

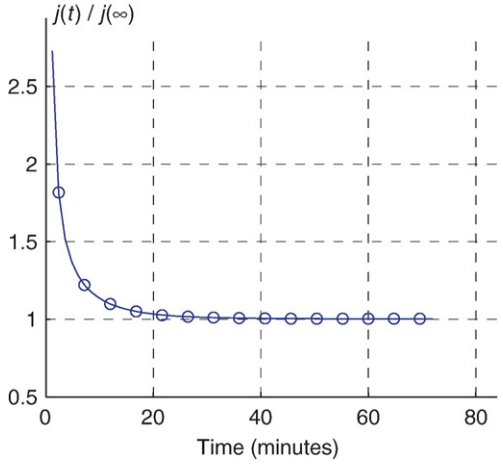

Fig. 6. Chloride flux at downstream chamber as ratio of steady-state flux for truly accelerated migration test.

8. Analysis of Friedmann et al. data

In the following we analyze the migration experiment of Friedmann et al. [24] summarized in Table 3.

The results of Friedmann et al. are given in Table 4. The diffusivities D_{FR1} and D_{FR2} were computed on the basis of electric current intensity measurements, $D^{\mathrm{flux,exp}}_{\mathrm{SSM}}$ is given by (11), whereas $D^{\mathrm{flux,exp}}_{\mathrm{PNP}}$ can be computed from (35). As seen, there is some scatter in the results with the diffusivities of Friedmann et al. exceeding those computed from steady state flux measurements. Also given in [24] is a plot of the cumulative chloride content in the downstream compartment. The data points from this figure (Fig. 2 in [24]) have been read off and attempted fitted using the complete PNP equations. The effective diffusivities were taken as

$$D_{\mathrm{Na}} = \frac{\mathcal{D}_{\mathrm{Na}}}{\mathcal{D}_{\mathrm{Cl}}} D_{\mathrm{Cl}}, D_K = \frac{\mathcal{D}_K}{\mathcal{D}_{\mathrm{Cl}}} D_{\mathrm{Cl}}, D_{\mathrm{OH}} = \frac{\mathcal{D}_{\mathrm{OH}}}{\mathcal{D}_{\mathrm{Cl}}} D_{\mathrm{Cl}} \tag{50}$$

where $\mathcal{D}_{\mathrm{Cl}} = 2.03\times10^{-9}$ m^2/s, $\mathcal{D}_{\mathrm{Na}} = 1.33\times10^{-9}$ m^2/s, $\mathcal{D}_K = 1.96\times10^{-9}$ m^2/s, $\mathcal{D}_{\mathrm{OH}} = 5.26\times10^{-9}$ m^2/s are the self-diffusion coefficients of the respective ions. The exercise thus consists of determining D_{Cl} so as to obtain the best possible fit to the experimental results. This task has been carried out by eye and using trial and error calculations. The results can be seen in Fig. 7. In view of the fact that there is some uncertainty in the measurement of the chloride concentration in the downstream compartment [24], the agreement between theory and experiment

Table 3
Setup used for experimental studies by Friedmann et al. [24]

c_0^{Na}	c_0^{K}	c_0^{OH}	c_0^{Cl}	c_l^{Na}	c_l^{K}	c_l^{OH}	c_l^{Cl}	l[mm]	$\Delta\phi$[V]
0.525	0.083	0.108	0.500	0.025	0.083	0.108	0.000	10	3

All concentrations are in mol/L.

Table 4
Results of Friedmann et al. [24] together with results of re-analysis

	$w/c=0.3$	$w/c=0.5$	$w/c=0.7$	Units
j_{meas}	13.5	18.1	33.5	$[10^{-6}$ mol/m^2/s$]$
D_{FR1}	12.6	24.7	30.5	$[10^{-12}$ m^2/s$]$
D_{FR2}	13.4	19.5	25.6	$[10^{-12}$ m^2/s$]$
$D_{SSM}^{flux,exp}$	2.31	3.10	5.73	$[10^{-12}$ m^2/s$]$
$D_{PNP}^{flux,exp}$	4.85	6.51	12.0	$[10^{-12}$ m^2/s$]$
D_{PNP}^{fit}	11.0	14.5	23.5	$[10^{-12}$ m^2/s$]$

is very good. The diffusivities that fit the experimental data are given in Table 4 as D_{PNP}^{fit}.

We see that these are somewhat smaller than those suggested by Friedmann et al. [24]. Also, on inspecting the experiment in more detail, we find that a steady state is far from attained at the time Friedmann et al. indicate that it is broken off (after some 150 h). The chloride flux in the downstream compartment as function of time is shown in Fig. 8 for the $w/c=0.5$ paste. As we can see, the flux at 150 h in only around 60% of the steady state flux. Thus, from this analysis we can conclude that it is likely that steady state diffusivities identical to those found from fitting the results in Fig. 7 would have been found, had Friedman et al. let the experiment run until a true steady state had been attained.

To conclude the analysis, we examine the effect of decreasing the effective sodium diffusivity. Goto and Roy [1] found a diminished mobility of this ion and hypothesized that this was caused by the influence of electric double layers. In the present we may account for the diminished mobility in a phenomenological manner by reducing the effective sodium diffusivity as

$$D_{Na} = \beta \frac{\mathcal{D}_{Na}}{\mathcal{D}_{Cl}} \mathcal{D}_{Cl} \tag{51}$$

where $\beta \leq 1$ is a phenomenological constant. Again, we attempt to find the optimal effective chloride diffusivities, i.e. those which, with the reduced sodium diffusivity, fit the experimental data best. The results of these curve fits can be seen in Fig. 9 and

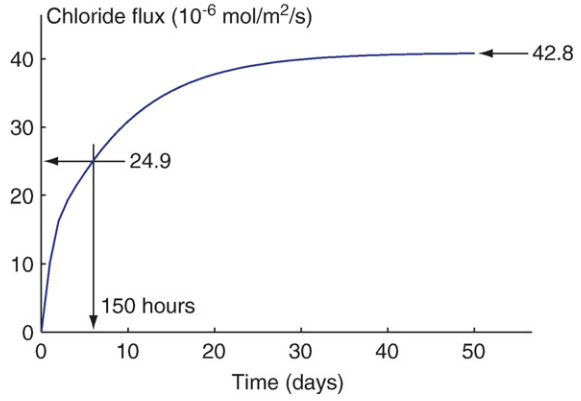

Fig. 8. Re-analysis of Friedmann et al. [24] data. Flux into downstream compartment as function of time.

the corresponding effective diffusivities are given in Table 5. As seen, the fits are still very good (perhaps even better) and the chloride diffusivities need only to be altered slightly. Thus, even though the microscopic physical mechanism behind the reduced sodium mobility may be very complex, it is still entirely possible that meaningful results may be obtained from the macroscopic PNP equations.

9. Conclusions

The conclusions are as follows:

- The complete steady-state Poisson–Nernst–Planck equations for an arbitrary number of monovalent ions are amenable to analytical solution under the assumption of electroneutrality, which in the context of the migration test is a reasonable assumption. All relevant quantities are given in the paper including a simple closed-form expression for the effective diffusivity.
- We have examined a number of common experimental setups and found that the difference in the effective diffusivities computed on the basis of the single-species model and the full PNP equations typically amount to

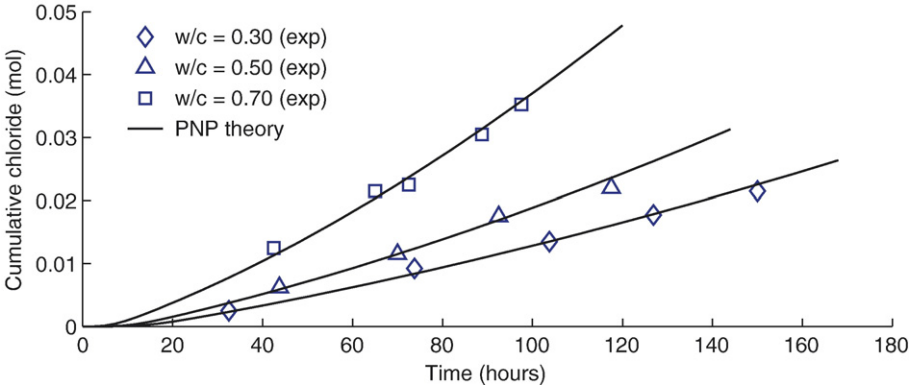

Fig. 7. Re-analysis of Friedmann et al. [24] data.

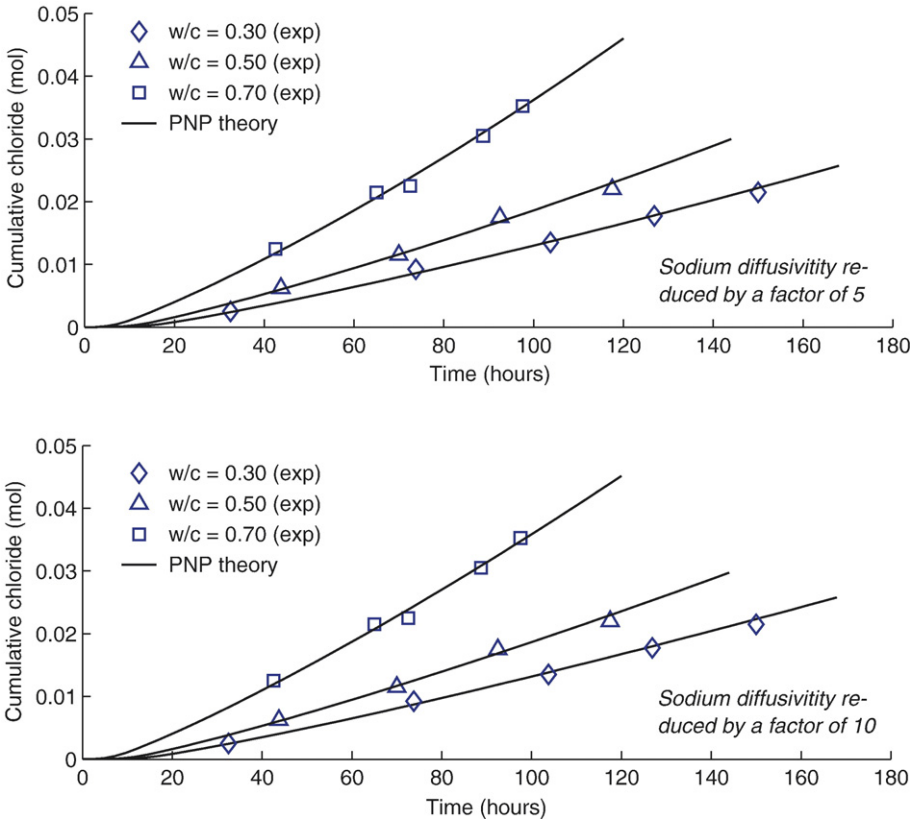

Fig. 9. Re-analysis of Friedmann et al. [24] data. Effect of reduced sodium diffusivity.

some 50 to 100%. However, for some setups the difference is of a more fundamental character, i.e. the PNP equations predict that the transport is due only to natural diffusion and that the imposed electric field has no influence.

- By properly designing the experiment, for example by adjusting the ratio of NaCl to NaOH, one can obtain a setup for which the conventional simplified model is reasonable. An experimental scheme where one would adjust this ratio, would also be well suited for verifying the validity of the PNP equations in describing the physical characteristics of the migration test.

Appendix A. Numerical solution of the PNP equations

In order to derive a numerical solution scheme we will, for the sake of simplicity, consider only the case of two monovalent ions. In this case the governing equations are

$$\frac{\partial c^+}{dt} - \frac{\partial^2 c^+}{\partial x^2} - k\frac{\partial}{\partial x}\left(c^+\frac{\partial \phi}{\partial x}\right) = 0 \tag{52}$$

$$\frac{\partial c^-}{dt} - \frac{\partial^2 c^-}{\partial x^2} + k\frac{\partial}{\partial x}\left(c^-\frac{\partial \phi}{\partial x}\right) = 0 \tag{53}$$

$$\epsilon\frac{\partial^2 \phi}{\partial x^2} + F(c^+ - c^-) = 0 \tag{54}$$

Using linear, two-node elements, standard finite element discretization procedures (see e.g. [25]) lead to a system of nonlinear equations given by

$$r = \overline{\boldsymbol{M}}\frac{\mathrm{d}\phi}{\mathrm{d}x} + \overline{\boldsymbol{K}}x + q = 0 \tag{55}$$

Table 5
Re-analysis of Friedman et al. [24] data

	$w/c=0.3$	$w/c=0.5$	$w/c=0.7$	Units
$D^{\mathrm{fit}}_{\mathrm{PNP}}$, $\beta=1$	11.00	14.50	23.5	$[10^{-12}$ m^2/s]
$D^{\mathrm{fit}}_{\mathrm{PNP}}$, $\beta=1/5$	11.25	14.75	24.5	$[10^{-12}$ m^2/s]
$D^{\mathrm{fit}}_{\mathrm{PNP}}$, $\beta=1/10$	11.50	15.00	25.0	$[10^{-12}$ m^2/s]

Effective chloride diffusivities computed by fitting experimental data. Effect of reduced sodium diffusivity.

Table 6
Experimental setups for validating the electroneutrality approximation

	$c_{\mathrm{Na},0}$	$c_{\mathrm{K},0}$	$c_{\mathrm{OH},0}$	$c_{\mathrm{Cl},0}$	$c_{\mathrm{Na},1}$	$c_{\mathrm{K},1}$	$c_{\mathrm{OH},1}$	$c_{\mathrm{Cl},1}$	l[mm]	$\Delta\phi$[V]
Samson et al. [6]	800	0	300	500	300	0	300	0	35	14
Friedman et al. [24]	525	83	108	500	25	83	108	0	10	3
McGrath (6 V) [18]	800	0	300	500	300	0	300	0	30	6
McGrath (30 V) [18]	800	0	300	500	300	0	300	0	30	30

All concentrations are in mmol/L.

Table 7
Test of the validity of the electroneutrality assumption on four different experimental setups

	Samson et al.	Friedman et al.	McGrath (6 V)	McGrath (30 V)
ϵ(F/m)	j_{numer}/j_{analyt}	j_{numer}/j_{analyt}	j_{numer}/j_{analyt}	j_{numer}/j_{analyt}
1e−01	0.84360	0.74138	0.88190	0.84995
1e−02	0.91225	0.77281	0.96414	0.84323
1e−03	0.98275	0.93045	0.99533	0.93090
1e−04	0.99806	0.99045	0.99952	0.98864
1e−05	0.99980	0.99900	0.99995	0.99878
1e−06	0.99997	0.99990	1.00000	0.99988
1e−07	1.00000	0.99999	1.00000	0.99999
1e−08	1.00000	1.00000	1.00000	1.00000

The fluxes j_{analyt} are calculated from (33). The permittivities in the first column may be compared to that of water at room temperature: $\epsilon_{water} \simeq 7\times10^{-10}$ F/m.

where q accounts for the boundary conditions and

$$\overline{\boldsymbol{M}} = \begin{bmatrix} M & 0 & 0 \\ 0 & M & 0 \\ 0 & 0 & 0 \end{bmatrix}, \overline{\boldsymbol{K}} = \begin{bmatrix} K & 0 & G^+ \\ 0 & K & G^- \\ Z^+ & Z^- & H \end{bmatrix}, \quad x = \begin{bmatrix} c^+ \\ c^- \\ \phi \end{bmatrix} \tag{56}$$

The individual element contributions are given by

$$\boldsymbol{M}_e = \frac{l}{6}\begin{bmatrix} 2 & 1 \\ 1 & 2 \end{bmatrix}, \boldsymbol{K}_e = \frac{1}{l}\begin{bmatrix} 1 & -1 \\ -1 & 1 \end{bmatrix}, \quad \boldsymbol{Z}_e^{\pm} = \pm\frac{l}{6}F\begin{bmatrix} 2 & 1 \\ 1 & 2 \end{bmatrix} \tag{57}$$

$$\boldsymbol{G}_e^{\pm} = \pm k\boldsymbol{A}_e c_e^{\pm}\boldsymbol{K}_e, \quad \boldsymbol{H}_e = \epsilon\boldsymbol{K}_e \tag{58}$$

where $\boldsymbol{A}_e$ is a weighting matrix, for example $\boldsymbol{A}_e = \left[\frac{1}{2}, \frac{1}{2}\right]$. In some cases it may be prudent to use upstream weighting or similar techniques derived from fluid mechanics. Otherwise, in order to avoid non-physical oscillations, it is advisable to refine the mesh near the boundaries. Also, it is possible to use both lumped and consistent versions of the matrices $\boldsymbol{M}$ and $\boldsymbol{Z}^{\pm}$. Using the backward Euler scheme, the equations are discretized in time as

$$r_{n+1} = \overline{\boldsymbol{M}}(x_{n+1} - x_n) + \Delta t\,\overline{\boldsymbol{K}}_{n+1}x_{n+1} + \Delta t q = 0 \tag{59}$$

The nonlinear equations are solved iteratively using Newton's method. This gives the following iterative scheme

$$\delta x = -\left(J_n^j\right)^{-1} r_{n+1}^j, \quad x_{n+1}^{j+1} = x_{n+1}^{j+1} + \delta x \tag{60}$$

where j counts iterations (these are initiated from the last converged point, i.e. $x_{n+1}^0 = x_n$). This proceeds until $\|\delta x\| \le \varepsilon$ where $\varepsilon \simeq 10^{-9}$. The Jacobian is given by

$$\boldsymbol{J} = \overline{\boldsymbol{M}} + \Delta t\left(\overline{\boldsymbol{K}} + \overline{\boldsymbol{K}}_g\right) \tag{61}$$

where

$$\overline{\boldsymbol{K}}_g = \begin{bmatrix} \boldsymbol{K}_g^+ & 0 & 0 \\ 0 & \boldsymbol{K}_g^- & 0 \\ 0 & 0 & 0 \end{bmatrix} \tag{62}$$

with the individual element contributions of $\boldsymbol{K}_g^{\pm}$ being given by

$$\left(\boldsymbol{K}_g\right)_e^{\pm} = \pm k\boldsymbol{K}_e\phi_e\boldsymbol{A}_e \tag{63}$$

The numerical scheme described above has been implemented for an arbitrary number of ions (not necessarily monovalent) and can thus be used to verify the validity of the electroneutrality assumption. To do this we consider four experimental setups as summarized in Table 6. These problems are solved for a decreasing sequence of permittivities and the results (in terms of the steady state fluxes) are listed in Table 7. As seen, the electroneutrality assumption is for these realistic experimental setups validated.

Finally, the concentration profiles and the electric potential distribution for the setup used by Friedman et al. [24] are shown

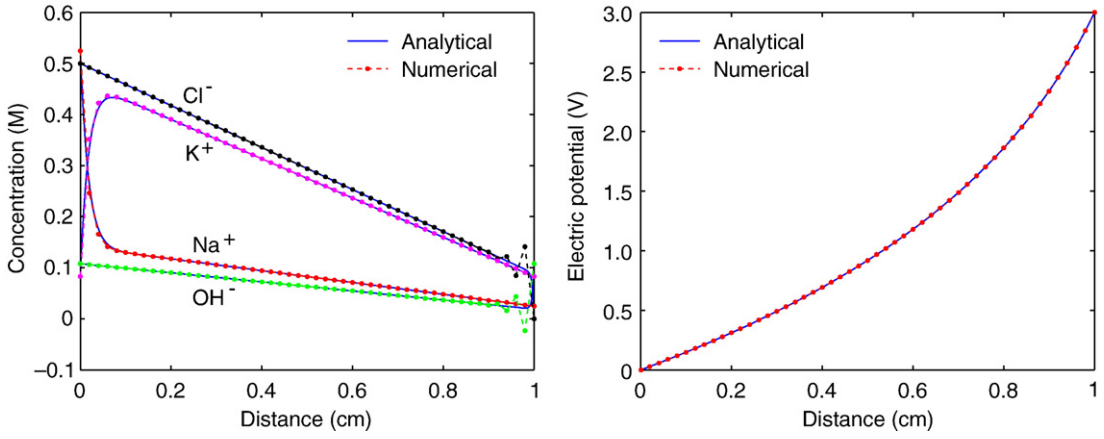

Fig. 10. Steady state concentrations (left) and electric potential distribution (right) for Friedman et al. test (see Table 3). The numerical results were computed using a 50 finite element mesh.

in Fig. 10. We see that the agreement between the numerical and analytical solutions is quite good except at the right end of the sample where the numerical solution displays nonphysical oscillations (which will eventually disappear as the mesh is refined).

References

[1] S. Goto, D.M. Roy, Diffusion of ions through hardened cement pastes, Cement and Concrete Research 11 (1981) 751–757.

[2] C. Andrade, Calculation of chloride diffusion coefficients in concrete from ionic migration measurements, Cement and Concrete Research 23 (1993) 724–742.

[3] C. Andrade, M.A. Sanjuan, A. Recuero, O. Rio, Calculation of chloride diffusion coefficients in concrete from migration experiments, in non steady-state conditions, Cement and Concrete Research 24 (1994) 1214–1228.

[4] E. Samson, J. Marchand, J.L. Robert, J.P. Bournazel, Modelling of ion diffusion mechanisms in porous media, International Journal for Numerical Methods in Engineering 46 (1999) 2043–2060.

[5] E. Samson, J. Marchand, J.J. Beaudoin, Describing ion diffusion mechanisms in cement-based materials using the homogenization technique, Cement and Concrete Research 29 (1999) 1341–1345.

[6] E. Samson, J. Marchand, K.A. Snyder, Calculation of ionic diffusion coefficients on the basis of migration test results, Materials and Structures 36 (2003) 156–165.

[7] O. Truc, J.P. Ollivier, L.O. Nilsson, Numerical simulation of multi-species transport through saturated concrete during a migration test–MsDiff code, Cement and Concrete Research 30 (2000) 1581–1592.

[8] S.W. Yu, C.L. Page, Diffusion in cementitious materials: 1. Comparative study of chloride and oxygen diffusion in hydrated cement pastes, Cement and Concrete Research 21 (1991) 581–588.

[9] V.T. Ngala, et al., Diffusion in cementitious materials: II. Further investigations of chloride and oxygen diffusion in well-cured OPC and OPC/30% PFA pastes, Cement and Concrete Research 25 (1995) 819–826.

[10] D.E. Goldman, Potential, impedance, and rectification in membranes, Journal of General Physiology 27 (1943) 37–60.

[11] M. Castellote, C. Andrade, C. Alonso, C.L. Page, Oxygen and chloride diffusion in cement pastes as a validation of chloride diffusion coefficients obtained by steady-state migration tests, Cement and Concrete Research 31 (2001) 621–625.

[12] A. Xu, S. Chandra, A discussion of the paper" calculation of chloride diffusion coefficients in concrete from ionic migration measurements" by C. Andrade, Cement and Concrete Research 24 (1994) 375–379.

[13] A.D. MacGillivray, Nernst-Planck equations and the electroneutrality and Donnan equilibrium assumptions, Journal of Chemical Physics 48 (1968) 2903–2907.

[14] B.F. Johannesson, Diffusion of a mixture of cations and anions dissolved in water, Cement and Concrete Research 29 (1999) 1261–1270.

[15] E. Cussler, Diffusion Mass Transfer in Fluid Systems, Cambridge University Press, 1974.

[16] M. Castellote, C. Andrade, C. Alonso, Measurement of the steady and non-steady-state chloride diffusion coefficients in a migration test by means of monitoring the conductivity in the anolyte chamber. Comparison with natural diffusion tests, Cement and Concrete Research 31 (2001) 1411–1420.

[17] L. Tang, L.O. Nilsson, Rapid determination of the chloride diffusivity in concrete by applying an electric field, Cement and Concrete Research 89 (1992) 49–53.

[18] P.F. McGrath, R.D. Hooton, Influence of voltage on chloride diffusion coefficients from chloride migration tests, Cement and Concrete Research 26 (1996) 1239–1244.

[19] L. Tang, L.O. Nilsson, A discussion on the paper Calculation of chloride diffusion coefficients in concrete from migration experiments, in non steady-state conditions" by C. Andrade, M.A. Sanjuan, A. Recuero and O. Rio, Cement and Concrete Research 25 (1995) 1133–1137.

[20] L. Tang, Chloride transport in concrete – measurement and prediction, Ph.D. thesis, Chalmers University of Technology, Gotheburg, Sweden (1996).

[21] K. Stanish, R.D. Hooton, M.D.A. Thomas, A novel method for describing chloride ion transport due to an electrical gradient in concrete: Part1. Theoretical description, Cement and Concrete Research 34 (2004) 2251–2260.

[22] G. Bramhall, The validity of Darcy's law in the axial penetration of wood, Wood Science and Technology 5 (1971) 121–134.

[23] K. Krabbenhoft, L. Damkilde, Double porosity models for the description of water infiltration in wood, Wood Science and Technology 38 (2004) 641–659.

[24] H. Friedmann, O. Amiri, A. Ait-Mokhtar, P. Dumargue, A direct method for determining chloride diffusion coefficient by using migration test, Cement and Concrete Research 34 (2004) 1967–1973.

[25] R.W. Lewis, K. Morgan, H.R. Thomas, K.N. Seetharamu, The Finite Element Method in Heat Transfer Analysis, John Wiley & Sons, New York, 1996.